Wacker-oxidation of Ethylene over Pillared Layered Material Catalysts

Róbert Barthos[*], *András Hegyessy, Zoltán May, József Valyon*
Institute of Materials and Environmental Chemistry, Research Centre for Natural Sciences, Hungarian Academy of Sciences, Pusztaszeri út 59-67, Budapest 1025, Hungary
*Corresponding author. Tel:+36 1 4381130; fax:+36 1 4381164
E-mail addresses: barthos.robert@ttk.mta.hu (Róbert Barthos), hegyessy@gmail.com (András Hegyessy), may.zoltan@ttk.mta.hu (Zoltán May), valyon.jozsef@ttk.mta.hu (József Valyon)

Abstract

This paper concerns the Wacker oxidation of ethylene by oxygen in the presence of water over supported Pd/VO_x catalysts. High surface area porous supports were obtained from layer-structured materials, such as, montmorillonite (MT), laponite (LT) (smectites), and hydrotalcite (layered double hydroxide, LDH) by pillaring. Before introduction of Pd, supports MT and LDH were pillared by vanadia. The laponite was used in titania-pillared form (TiO_2-LAP) as support of Pd/VO_x active component. Acetaldehyde (AcH), acetic acid (AcOH) and CO_2 were the products with yields and selectivities, depending on the reaction conditions and the properties of the applied catalyst. Under comparable conditions the pillared smectite catalysts gave higher AcH yield than the pillared LDH catalyst. UV-vis spectroscopic examination suggested that the pillared smectites contained polymeric chains of VO_4, whereas only isolated monomeric VO_4 species were present in the pillared LDH. The higher catalytic activity in the Wacker oxidation was attributed to the more favorable redox property of the polymeric than of the monomeric vanadia. The V^{3+} ions in the polymeric species can reduce O_2 to O^{2-} ions, whereas the obtained V^{5+} ions are ready to pass over O to Pd^0 to generate PdO whereon the oxidation of the ethylene proceeds.

Keywords: Wacker oxidation · Supported Pd/VO_x catalyst · Pillared layered materials · UV-VIS spectroscopy H_2-TPR

1 Introduction

Acetaldehyde is a commodity chemical. By the end of the last century the world's production of acetaldehyde attained 2.9 million tons/year. About 85% of this amount was

manufactured in plants exploiting the method, patented by the Wacker and Hoechst companies in 1959. The process involves bubbling mixture of ethylene and oxygen (air) through aqueous solution of homogeneous catalyst consisting of HCl, $PdCl_2$ and $CuCl_2$. In the first step of the reaction Pd^{2+} cations promote the nucleophyllic attack of alkene by water, the ethylene takes up an oxygen atom, and the Pd^{2+} gets reduced to Pd^0. The role of co-catalyst Cu^{2+} ions is to selectively re-oxidize the Pd^0 to Pd^{2+}. The catalytic cycle is closed by the re-oxidation of the resulting Cu^+ by O_2 [1]. However, the liquid-phase homogeneous process has many disadvantages, such as the high corrosivity of HCl in the presence of oxygen, possible formation of undesired chlorinated by-products, difficult recovery of the products from solution, loss of palladium, etc. A solid catalyst that functions like the homogeneous catalytic system could overcome most of these drawbacks [2].

There have been a number of attempts to heterogenize the homogeneous Wacker catalyst system by binding an active complex onto a carrier material and, thereby, combine the advantages of the homogeneous and heterogeneous catalysts. Various oxides (Al_2O_3, SiO_2, TiO_2) [3-6] and carbon[7,8] were used as support. In these systems either vanadia [3-5] or copper [67-8] was the co-catalyst of palladium. Espeel et al.[9] used Cu-Pd exchanged Y zeolites to initiate selective AcH formation in the reaction of ethylene and oxygen. Terminal oxidation of alpha olefins was attained using Pd-MT catalyst in acid-free aqueous solution of $CuCl_2$ and *N*,*N*-dimethylacetamide [10]. Porous glass was used by Arhancet [11] to adsorb palladium and copper salts and generate, thereby, a heterogenized Wacker-system. Recently active palladium/copper chloride composition, fixed to silica-supported liquid polymer medium, was used to make AcH by selective vapor phase oxidation of ethylene 12].

With the objective of mitigating some engineering problems of the Wacker reaction a membrane reactor was developed by Frusteri et al. [13]. A Pd or Pt/carbon membrane was applied to separate an oxidizing liquid phase and a gas flow containing the reactant ethylene. The reaction was accompanied by a continuous countercurrant transport of the reactant and the products through the catalytically active membrane.

The present study shows that active heterogeneous Wacker type catalyst can be prepared by depositing Pd on vanadia-pillared layered materials, such as, smectites and LDH.

2 Experimental

2.1 Preparation of catalysts

Smectite layers comprise of two tetrahedral SiO_4 sheets sandwiching an octahedral AlO_4 sheet. Substitution of some Al^{3+} to Mg^{2+} or Li^+ raises a negative charge on the layers, compensated by hydrated cations in the interlayer region. The interlayer ions can be exchanged by VO^{2+} cations [14]. When the ion exchanged samples are subject of careful thermal treatment dehydration and dehydroxylation occur and highly dispersed V_2O_5 particles are formed, which keep the layers apart like pillars.

As a first step of making vanadia-pillared montmorillonite (VO_x-MT) 10 g of montmorillonite K-10 (Aldrich) was suspended in 1000 cm^3 distilled water at 50 °C by intense stirring of the mixture for 4 h. Then, 500 cm^3 solution, having a vanadyl sulfate (Sigma-Aldrich, 97 % purity) concentration of 0.02 mol/dm^3, was added to the stirred suspension dropwise. The amount of added $VOSO_4$ (10 mmol) was near to equivalent with the ion exchange capacity(IEC) of the used MT (12 mmol/10 g). After additional 16-hour stirring at 50 °C the suspension was filtered, the obtained solid was washed with distilled water, and dried in air at 120 °C overnight. The dried material was calcined at 400 °C for 4 h. The chemical analysis of the sample showed that 37 % of the vanadium moved from the exchange solution into the MT structure. This amount corresponds to about 30 % of the IEC of the MT.

The laponite (LT) is synthetic structural analogue of hectorite. The LT sample (XLG, Rockwood Ltd.) was pillared twice: first with titania (TiO_2-LT) and then with vanadia (VO_x-TiO_2-LT) as described by Long et al. [14]. The Ti was introduced from an aqueous solution, containing $TiCl_4$ and HCl in concentrations of 0.94 and 0.66 mol/dm^3, respectively. Ten grams of LT was suspended in 1000 cm^3 water and slowly 110 cm^3 of the solution was added to it in drops. The amount of added $TiCl_4$ (104 mmol) was about ten times as much as the ion exchange capacity of the used laponite (10 mmol/10 g). The particles separated from the liquid phase were dried at 120 ^oC overnight. The dried sample was calcined at 400 ^oC for 4 h. The chemical analysis showed that close 90 % of the added Ti (90 mmol) remained in the solid in the form of titania.

The procedure, the treatments and the conditions of vanadia introduction in the TiO_2-LT were similar to that described above for the MT sample. The amount of vanadium, moved from the $VOSO_4$ solution into the TiO_2-LT structure was about 37 % of the total IEC of the LP sample.

The LDHs, known also as hydrotalcites, consist of brucite [$Mg(OH)_2$]-like layers wherein a fraction of the divalent magnesium cations is substituted by trivalent ions. As a result, the layers get positive charge, which is balanced by hydrated anions in the interlayer space. The

interlamellar ions can be exchanged by decavanadate, $V_{10}O_{28}^{6-}$, anions. Thermal treatment of the ion-exchanged material must be applied to obtain the vanadia pillared hydrotalcite.

A VO_x-LDH sample was prepared following the receipt described by Wegrzyn et al.[15]. First LDH was made by mixing a Mg^{2+}/Al^{3+} solution (2 to 1 Mg/Al molar ratio) and a solution containing CO_3^{2-} ions at 60 °C. Namely, 0.2 mol magnesium nitrate hexahydrate (99 % purity, Sigma-Aldrich) and 0.1 mol aluminium nitrate nonahydrate (98+% purity, Sigma-Aldrich) was dissolved in 200 cm^3 water and added in drops to 60 mmol sodium carbonate, dissolved in 100 cm^3 water. During addition of the nitrate solution the pH of the obtained slurry was kept at 10±0.2 by gradual addition of 3.2 M NaOH solution. After having full amounts of the solutions combined the slurry was stirred at 60 °C for 1 h. The interlayer carbonate anions were exchanged then by decavanadate ($V_{10}O_{28}^{6-}$) solution. The solution was made by dissolving 12.193 g $NaVO_3$ (Aldrich, 99.9%) in 360 ml water at pH= 4.5. The pH was adjusted using 1 M HNO_3 solution. The ion-exchange was carried out at pH=4.5±0.1 and was accomplished in 5 min. Afterwards the suspension was filtered, washed by distilled water, dried at 110^{o}C overnight and calcined then at 300 °C for 4 hours to get VO_x-LDH sample. The negative charge of the used decavanadate was near to equivalent with half of the ion-exchange capacity of the used LDH sample. The chemical analysis of the calcined sample showed that virtually the total vanadium content of the exchange solution became incorporated into the LDH structure.

Using $Pd(NH_3)_4(NO_3)_2$ (Strem Chemicals Inc.) a solution was made containing 5 wt % Pd. Catalysts of about 0.6-0.8 wt% Pd content were obtained by impregnating the above described supported vanadia preparations with the solution and calcining them at 300 °C (VO_x-LDH) or 400 °C(VO_x-MT and VO_x-TiO_2-LT) for 4 hours. The catalysts were designated as Pd/VO_x-MT, Pd/VO_x-TiO_2-LT, and Pd/VO_x-LDH.

2.2 Characterization

A Philips PW 1810/3710 X-ray diffractometer, applying monochromatized CuK_α radiation (40 kV, 35 mA) was used. The XRD patterns of the samples (Fig. 1) were recorded at ambient conditions collecting data between 3° and 65° 2Θ degrees in 0.02° steps for 0.5 s at each step.

Nitrogen physisorption measurements were carried out at -195 °C using Quantachrome NOVA Automated Gas Sorption Instrument. Prior to measurements the samples were outgassed at 150 °C for 8 h. The specific surface area (SSA) values were calculated by the BET method from seven measured points of the N_2 adsorption isotherm recorded in the relative pressure interval from 0.05 to 0.35 at -195 ^{o}C (Table 1.

.

The morphology of the preparations (Fig. 2) was examined by Morgagni 268D Transmission Electron Microscope (100 kV, W filament, point resolution = 0.5 nm)

The palladium and vanadium content of samples (Table 1) was determined by means of ICP-OES sequential plasma emission spectrometer with radial plasma viewing (Thermo Jarrell Ash, AtomScan 25 type).

Temperature-programmed reduction measurements were carried out by hydrogen (H_2-TPR) using a flow-through microreactor (I.D. 4 mm) made of quartz. About 100 mg of catalyst sample (particle size: 0.25–0.5 mm) was placed into the microreactor and was pre-treated in a 30 cm^3/min flow of O_2 at 350 °C for 1 h before the measurement. The pre-treated sample was cooled to room temperature in the O_2 flow, flushed by N_2 at room temperature for 30 min then was contacted with a 30 cm^3/min flow of 10% H_2/N_2 mixture. The reactor temperature was ramped up at a rate of 10 °C/min to 600 °C and held at this temperature for 1h, while the effluent gas was passed through a liquid nitrogen trap and a thermal conductivity detector (TCD). Data were collected and processed by computer. Calculation of the corresponding hydrogen consumptions based on the peak areas was carried out by using the calibration value determined with the H_2-TPR of CuO reference material. The reducibility of the catalysts was characterized by the molar hydrogen consumption of the PdO and the VO_x phases. The VO_x reducibility of the VO_x-MT and VO_x-TiO_2-LT samples were obtained by correcting the total hydrogen consumption of the samples with the hydrogen consumption of the MT and TiO_2-LT support, respectively, determined in separate TPR experiments. Similar correction was applied to obtain the extent of palladium reduction in the Pd/MT and Pd/TiO_2-LT samples. In order to obtain the extent of VO_x reduction in the Pd/VO_x-MT and Pd/VO_x-TiO_2-LT catalysts the H_2 consumptions obtained for the Pd/MT and Pd/TiO_2-LT samples was taken in correction (Fig. 3 and Table 2).

A tapered element oscillating microbalance (TEOM 1500 Pulse Mass Analyzer from Rupprecht & Patashnick Co.) was used to determine the CO chemisorption of the pre-reduced Pd-containing catalysts. About 100 mg of catalyst sample was reduced in flowing H_2 at 300 °C (Pd/VO_x-LDH) or 400 °C (Pd/VO_x-TiO_2-LT; Pd/VO_x-MT), flushed by He at the reduction temperature for 60 min then cooled to 40°C. After having a stabilized weight monitored for about for 3 h, the sample was contacted with a flow of 3% CO/He for 60 min at 40°C followed by a repeated flushing with He for 60 min at the same temperature. The chemisorbed amount of CO was determined as difference of the weights recorded in He flow before after contacting the catalyst with CO.

UV-vis spectra of the preparations were collected by Thermo Scientific Evolution 300 UV-VIS spectrophotometer equipped with Praying Mantis Diffuse Reflectance Accessory and High Temperature and Pressure Reaction Chamber, allowing in situ measurements of powdered solids (in situ DR-UV-vis). The reference materials ($NaVO_3$, 99.9%, Na_3VO_4 99.98%, Sigma-Aldrich products) and all the studied preparations were finely ground and diluted with $BaSO_4$ (Alfa Aesar, Puratronic 99,998%). The DR-UV-vis spectra were measured against $BaSO_4$ as background. The dilution was applied to get Kubelka-Munk function $F(R\infty) < 1$. In order to obtain spectra of dehydrated samples both the background and absorbance data were collected at 350 °C after *in-situ* calcination at 350 °C in flowing oxygen for 30 min. The edge energy (E_g) for allowed transitions were obtained as the intercept of the straight line fitted to the low-energy rise of the $[F(R\infty) \times h\nu]^2$ vs. hν plot (Fig. 4) as described in refs. [16,17].

2.3 Catalytic activity measurements

The catalyst preparations were characterized by their activity and selectivity in the Wacker oxidation of ethylene (Fig 5). In the reaction 500 mg of catalyst sample (particle size 0.85-1.70 mm) was used at atmospheric pressure in a fixed-bed continuous flow glass tube reactor, having an internal diameter of 4 mm. The catalyst was activated in situ in the reactor in oxygen flow (20 cm^3/min) at 350°C for 1 h then contacted with a gas flow of 3% C_2H_4/12% O_2/24% H_2O/He at a total flow rate of 30 cm^3/min. The reactor effluent was analyzed by an on-line Shimadzu GC-2010 gas chromatograph equipped with automatic gas sampling valve and 30-m long HP-PLOT-U column. On each temperature the reaction was followed for 5 hours. Flame-ionization detector (FID) was used to detect the main organic compounds, such as C_2H_4, AcH, AcOH, and the minor organic by-products, if any, whereas thermal conductivity detector (TCD) was applied to get signal from O_2, CO_2 and water. Between the reactor outlet and the GC the temperature of the gas line and the sampling valve was maintained at 120 °C in order to avoid the condensation of water and reaction products. The GC was calibrated for each reactant and product separately. The conversion of ethylene was calculated from the ethylene concentrations of the feed and the reactor effluent. The selectivities were calculated on the basis of the carbon content of the products. For instance, the acetaldehyde selectivity (S) was obtained as $S_{AcH}=2c_{AcH}/(2c_{AcH} + 2c_{AcOH} + c_{CO_2})$.

3 Results and discussion

The XRD patterns of the layered materials and their pillared derivatives are shown in Fig. 1.

The LDH has a hexagonal type unit cell. The XRD reflections were indexed using the ICDD card N^{o} 35-0965. The lattice parameters *c* and *a* were calculated from the position of the 003 and 110 reflections, respectively. For the parent LDH sample c=2.28 nm and a= 3.04 nm was obtained. After incorporation of vanadia species the 003, 006, and 009 reflections shifted to lower 2Θ values. Thus, the intercalation of decavanadate anions in the LDH brought about an increase in the interlayer distance from 0.76 to 0.98 nm. The position of 110 reflection did not change, indicating that the average cation-cation distance in the pillared octahedral, brucite-like sheets remained unaffected. The broad and weak reflections of the modified LDH sample indicate lattice disorder (Fig. 1A). Crystalline vanadia could not be detected despite of the relatively high vanadia content of the sample, suggesting high vanadia dispersion. Weak XRD lines belonging to hydrotalcite are also present after heat treatment at 300 °C (VO_x-LDH(a)). As Labajos et al. [18] demonstrated that distorted LDH structure is present after heat treatment at 275 °C, whereas appearance of MgO and Mg-Al-spinel structures were indicated only after treatment at 500 °C and above. The structural damage of our LDH sample is more pronounced, probably due to the affect of the acidic medium applied for ion exchange by $V_{10}O_{56}^{6-}$ ions. Heat treatment increased structural disorder but the LDH lines of the heat treated sample are still detectable (Fig. 1, see VO_x-LDH(a)).

In accordance with the finding of Long et al. [14] the introduction of vanadia in between the layers of the MT sample did not alter its XRD pattern (Fig. 1B). No vanadia reflections could be discerned. These findings may infer that calcination could not convert significant amount of the VO^{+} cations to VO_x species, alternatively, the VO_x, if formed, is present on the outer surface of the MT sample in highly dispersed form.

The strong acidic medium applied in the process of the titania-pillaring delaminated the LT sample as suggested by the much weaker LT reflections of the TiO_2-LT sample than those of the original LT sample (Fig. 1C). The weakening of the reflections is stronger than that explained by the presence of 39 wt % titania beside the LT phase. The weak XRD peaks of LT are accompanied by strong anatase reflections (ICDD Card No. 21-1272).

The SSA of the vanadia-containing sample was regularly smaller than the SSA of the corresponding support material having layered structure (Table 1). In contrast, the titania-pillared LT sample had a higher SSA than the LT phase alone. This finding suggests that delamination of the laponite phase occurred during the pillaring procedure. However, the

conversion of the TiO_2-LT to VO_x-TiO_2-LT by VO^{2+} cation exchange and subsequent calcination reduced the surface area as it happened with the other samples (Table 1).

No reflections of PdO or Pd^0 were found on the XRD patterns of the calcined catalysts, i. e., the XRD patterns of the VO_x and Pd/VO_x preparations were the same. The TEM images of the catalysts are shown in Fig. 2. The pillaring process and the palladium introduction did not significantly alter the morphology of the parent layered materials (not shown). Appearance of palladium metal particles was not expected and particles were not discerned since catalysts were not pre-reduced before the TEM examination.

According to present knowledge [19] the oxidation of the alkene proceeds with co-operation of V_2O_5, PdO and H_2O. In latter reaction AcH, AcOH, CO_2 products, Pd^0 and, most probably, V^{4+} is obtained. The alkene oxidation is accomplished in an oxygen transfer chain. The catalytic cycle proceeds if O_2 gas re-oxidizes the vanadium co-catalyst. The rate of any oxygen transfer step can determine the rate of oxidation reaction. If the oxidation/reduction rate of the vanadia was slow it could limit the rate of the Wacker oxidation reaction. The reducibility of supported VO_x and Pd/VO_x samples by hydrogen was used to characterize the oxygen/electron donor ability of the vanadia phase. Fig. 3 shows H_2-TPR profiles. The H_2 consumptions, calculated by integration of the H_2-TPR peaks, are given Table 2. The hydrogen consumption of the MT support (253 μmol/g) is much higher than that of the TiO_2-LT support (89 μmol/g). Unlike the LT, the MT, being of natural origin, contains reducible transition metal ions in an amount close to 2 wt %. The main component is iron (1.86 wt %). The palladium in the catalyst preparation increased the complexity of the reduction pattern. The reduction of palladium occurs at relatively low temperature (<~100 ^oC) where the generated Pd^0 particles adsorb hydrogen that is released at a somewhat higher but still at relatively low temperature (Fig. 3). Discern the small negative peaks on the TPR curves of the Pd-containing MT preparations below about 100 ^0C, indicating H_2 desorption from the palladium that must have been reduced in contact with hydrogen before the programmed temperature raise was started (Fig. 3B). The reduction of palladium over the LT containing preparations are somewhat hindered giving a sharp peak at about 100 ^oC. The reduced palladium can activate H_2 for the reduction of other reducible components shifting their reduction peaks to lower temperatures. This effect is more pronounced on the Pd/MT sample containing a significant amount of reducible transition metal than on the Pd/TiO_2-LT sample, containing only hard-to-reduce components like anatase and the pure synthetic smectite LT. The difference of the H_2 consumption of the Pd/MT and MT preparations was calculated. Because the palladium enhances reducibility (and became reduced before the experiment was

started) the difference in the H_2 consumption of the two materials probably reflects the affect of palladium on the reduction of metals in the MT support (Table 2). Similarly, the difference of the H_2 consumption of the Pd/ TiO_2-LT and TiO_2-LT preparations was also determined. Considering the low reducibility of the TiO_2-LT support, the difference allows the estimation of the H_2/Pd value. A value of 0.47 was obtained in line with expectations. The TPR results suggest that vanadia is most difficult to reduce in the LDH preparations, although the presence of palladium promotes its reducibility.

It is well documented that vanadia catalysts are active in oxidative dehydrogenation reactions at about 450 °C where vanadia can participate in redox processes [20]. The H_2-TPR results of the present work suggests that significant reduction of our supported VO_x catalysts could be attained above 400 °C. The reduction behavior of VO_x-MT and VO_x-TiO_2-LT samples was similar although the temperature, whereon the reduction was started, and the temperature of maximum reduction rate were somewhat lower for the latter sample (513 vs. 563 °C). In order to estimate the average oxidation state of the vanadium after the H_2-TPR experiment the reducibility of the support was taken in correction assuming that the H_2 consumption of the support was the same before and after vanadia introduction. Chemical analysis of the samples showed that the VO^+ ion exchange removed about 20 % of the iron that was present in the native MT support. As a consequence the H_2 consumption of the VO_x-MT sample was a bit over corrected, which led to a lower H_2/V ratio (H_2/V=0.62) than was the real value (Table 2). Because the support of the VO_x/TiO_2-LT sample hardly contains ions which were both exchangeable and reducible the correction for the H_2 uptake of the support is fairly applicable. The H_2/V values suggest that the formal average oxidation state of vanadium must be over both supports between V^{3+} and V^{4+} at the end of the H_2-TPR experiment (Table 2).

The DR UV-vis method is able to distinguish ortho and metavanadate compounds. The bulk orthovanadate (Na_3VO_4) and metavanadate ($NaVO_3$) compounds contain isolated VO_4 units and polymeric VO_4 chains, respectively [17]. The edge energy (E_g) of pure $NaVO_3$ sample was found to be 2.98 eV while that of Na_3VO_4 to 3.40 eV (Fig. 4). The intermediate E_g values of $NaVO_3$/Na_3VO_4 mechanical mixtures showed linear dependence on the molar ratio. That means that after generating an E_g vs. molar ratio calibration line the percentage of isolated and polymeric vanadia forms of the vanadia-containing catalysts can be obtained by determining the E_g edge energy.

Fig. 4 shows that the VO_x-LDH sample contains virtually the same vanadia species as Na_3VO_4, i.e., isolated VO_4 units (E_g = 3.38 eV). In contrast, the E_g values obtained for the

VO_x-MT and VO_x-TiO_2-LT samples were 3.22 and 3.16 eV, respectively, suggesting that these preparations contain mixtures of isolated VO_4 units and polymeric VO_4 chains. The redox properties of the vanadia component of the catalyst must have importance regarding the Wacker oxidation activity of the catalyst. The reducibility of vanadium atoms was found to depend on the polymerization level of vanadia [21]. The polymerized forms were shown to become more easily reduced than the isolated surface vanadia species. We can conclude that about 40 and 60 % of vanadia are present in polymeric form in the VO_x-MT and VO_x-TiO_2-LT samples, respectively. The H_2-TPR showed that the MT and TiO_2-LT supported VO_x shows similar reducibility suggesting that the supports are of similar character or, regarding reducibility, the interaction between the support and the polymeric vanadia species is of secondary importance.

As expected, the palladium was found to have pronounced effect on the reducibility of the VO_x in the supported Pd/VO_x catalysts. The H_2-TPR pattern of the Pd/VO_x-TiO_2-LT catalyst shows one sharp peak at 84 °C and a broad peak between 180 and 600 °C. In contrast, the H_2-TPR pattern of the Pd/VO_x-MT catalyst exhibits peaks at 94, 124 and 225 °C sitting on the top of a broad peak overarching the whole temperature range of the measurement. In order to get the reduction degree of vanadium the hydrogen consumption of the corresponding Pd-containing support was taken into correction. The average oxidation state of vanadium was between V^{2+} and V^{3+} in the Pd/VO_x-MT catalyst whereas it was between V^{3+} and V^{4+} in the Pd/VO_x-TiO_2-LT catalyst. These results suggest that in presence of Pd the vanadia is more easily and deeply reducible on the MT than on the TiO_2-LT support.

The results of catalytic test reactions are shown on Fig. 5. The main products, as expected, are AcH, AcOH and CO_2. Formation of methane and acetone was also detected with selectivities lower than about 1 %. Traces of propylene, acrolein and propionaldehyde were also discerned. It generally applies for all catalyst that, when the reaction temperature and conversion level is increased, the selectivity of AcH decreases, whereas the AcOH selectivity increases and the formation of CO_2 rapidly grows. The H_2-TPR curves show that the supported Pd/VO_x catalysts become partially reduced already at the low temperatures (< 200 ^oC) where the Wacker oxidation proceeds (Table 2). However, the oxidation state of the catalysts is significantly different. In the case of the MT supported catalyst the H_2 consumption can be associated with the reduction of V^{5+} (the PdO must have been reduced at lower temperature, out of the range of the measurement), whereas in the case of the TiO_2-LT supported catalyst virtually all the H_2 consumption comes from the reduction of the PdO component.

The reduction of the catalysts generates palladium particles on the support. The estimation of the average Pd particle size is generally determined by XRD using the Scherrer method or calculated from the dispersion, determined by H_2 or CO chemisorptions measurement [22,23]. In the present study the CO chemisorptions method was used to obtain the dispersion of palladium particles over the catalysts reduced by H_2 at 300 ^oC (Pd/VO_x-LDH) or 400 ^oC (Pd/VO_x-MT, Pd/VO_x-TiO_2-LT). It was assumed that the number of adsorbed CO molecules equals with the number of surface Pd atoms [22]. To calculate the particle diameter we used the 7.9×10^{-2} nm^2 value for the atomic surface area Pd and spherical particle model [22,23]. The obtained results are given in Table 1. Obviously support MT hinders less the aggregation of the reduced Pd atoms.

The Wacker oxidation proceeds in the presence of a reducing agent, the reactant ethylene, and the oxidizing agent O_2 that is in excess to the amount needed for the stoichiometric total oxidation of ethylene. The O_2 participates in a selective Wacker oxidation of ethylene to AcH and AcOH and in a non selective catalytic oxidation of the reactant and the organic products to CO_2. The average valence state of the working catalyst is determined by the relative rates of these reactions that in turn strongly depend on the temperature. The H_2-TPD results suggest that the oxide ions of the MT supported Pd/VO_x catalyst are more readily participate in redox processes that those of the TiO_2-LT catalyst. That may have relation to the catalytic activity and selectivity in the Wacker oxidation of ethylene. The ethylene conversion and the oxidation to CO_2 more rapidly increases with the increasing reaction temperature over the Pd/VO_x-TiO_2-LT catalyst than over Pd/VO_x-MT suggesting that the activation of the O_2 gas over the catalyst, having less mobile oxide ions, has a higher activation energy. As a consequence, the AcH selectivity rapidly drops as temperature is increased. Because of the opposite temperature dependence of conversion and AcH selectivity the AcH yield can be maximized by selecting the optimum reaction temperature.

The preparations, containing vanadia and no palladium, were not active in the oxidation of ethylene in the applied temperature range at all. When vanadium was absent the palladium on the support generated only carbon dioxide. These results prove that the Wacker mechanism, requiring both palladium and oxygen transfer co-catalyst, is effective in the partial oxidation of ethylene. The water is also important component of the process, however, if any oxidation proceeds water is formed. A minor amount of water in the reacting system could bring about the appearance of the Wacker products in minor amounts.

In spite of its highest vanadia content the lowest activity and AcH selectivity were obtained with the Pd/VO_x-LDH catalyst. The XRD results (Fig. 1A and Fig. 2) showed that

the original LDH structure was lost during vanadia introduction. The LDH framework is stable at pH>10, but the intercalation of $V_{10}O_{56}^{6-}$ had to be carried at pH=4.5. Both the low pH and the dehydroxylation during calcination could result in the degradation of LDH layers. The eventual fractional occlusion of vanadia could hinder its intimate contact with palladium particles. Nevertheless, the appearance of AcH product showed a low Wacker-type selective oxidation activity of the catalyst. A further probable reason of the low activity is that this catalyst contains mainly isolated vanadia species of lower oxygen mobility than that attributed to the oxygen atoms of polymeric vanadia. The vanadia must act as electron transmitter. The electrons over polymeric vanadia chains are much more delocalized so this vanadia form can more easily transmit oxygen atoms from oxygen molecule than isolated vanadia species.

Since the iron and vanadium content of montmorilloite samples is in the same range, the Pd/MT (without vanadium) was also checked in separate catalytic test reaction. This composition proved to be inactive in Wacker oxidation of ethylene, although Fe^{3+}/Fe^{2+} could serve as co-catalyst to Pd^0/Pd^{2+}, only formation of CO_2 was observed.

Preliminary studies showed that nanosized anatase particles are favorable support for the vanadia/palladium redox ensembles for getting active Wacker catalyst. This infers that the enhanced catalytic activity of Pd/VO_x-TiO_2-LT is probably associated with presence of TiO_2 nanoparticles. Further studies are needed to clarify the possible role of titania in the heterogeneous Wacker type selective oxidation catalysts.

4. Conclusions

It was attempted to introduce VO_x species as pillars between the layers of LDH and smectites. The vanadia-modified materials were used as support for palladium. The selective catalytic partial ethylene oxidation was shown to follow the Wacker mechanism over all samples. The catalysts containing polymericVO_4 species were more active than the one containin monomeric VO_4. The vanadia acts as electron transmitter. The electrons over polymeric vanadia chains are much more delocalized so this vanadia form can more easily transmit oxygen atoms from oxygen molecule than isolated vanadia species. The redox properties of the vanadia component were shown to be affected by the support-vanadia interaction and was significantly modified by the presence of palladium.

5. Acknowledgement

This work was financially supported by the Hungarian Scientific Research Fund (OTKA, contract no. K 100411).

Table1. Characterization of the supports and catalysts.

Sample ID[a]	**SSA, m^2/g**	**V_2O_5 (TiO_2), wt%**	**Pd, wt%**[b]	**D, %**[c]	**d_{Pd}**[d]**, nm**
VO_x-LDH (LDH)	108 (151)	40.0	0.59	31	4
VO_x-MT (MT)	210 (238)	3.35	0.69	9	13
TiO_2-LT (LT)	452 (320)	-			
VO_x-TiO_2-LT	365	3.35 (39.2)	0.85	29	4

[a] LDH=Layered Double Hydroxide, MT=K-10 montmorillonite, LT=Laponite.
[b]The amount of Pd introduced in the vanadia-pillared sample. The SSA of each Pd catalyst was about the same as that of its support.
[c] Pd-dispersity of the reduced catalyst. Calculated from CO chemsorption capacity. The number of the surface Pd atoms was taken as equal with the number of adsorbed CO molecules.
[d] The diameter of Pd particles was calculated with an area of 0.079 nm^2/Pd atom

Table2. Results derived from the H-TPR measurements of Fig. 3.

Sample ID	H_2 ($\mu mol/g_{cat}$)	H_2/V (H_2/Pd)
MT	253	-
Pd/MT	309	0.81[a]
VO_x-MT	484	>0.62
Pd/ VO_x-MT	781 (253[b] + 528[c])	1.28
TiO_2-LT	89	-
Pd/TiO_2-LT	129 (45[b]+84[c])	(0.47)
VO_x-TiO_2-LT	384	0.80
Pd/VO_x-TiO_2-LT	429 (139[b]+290[c])	0.81
Pd/LDH	97	-
VO_x-LDH	2046	0.83
Pd/VO_x-LDH	2275	0.92

[a] The difference of the H_2 consumption of Pd/MT and MT devided by the molar vanadium content. The number showes the Pd-induced reducibility increase of the MT support.
[b] H_2 uptake up to 200 ^oC.
[c] H_2 uptake from 200 ^oC up.

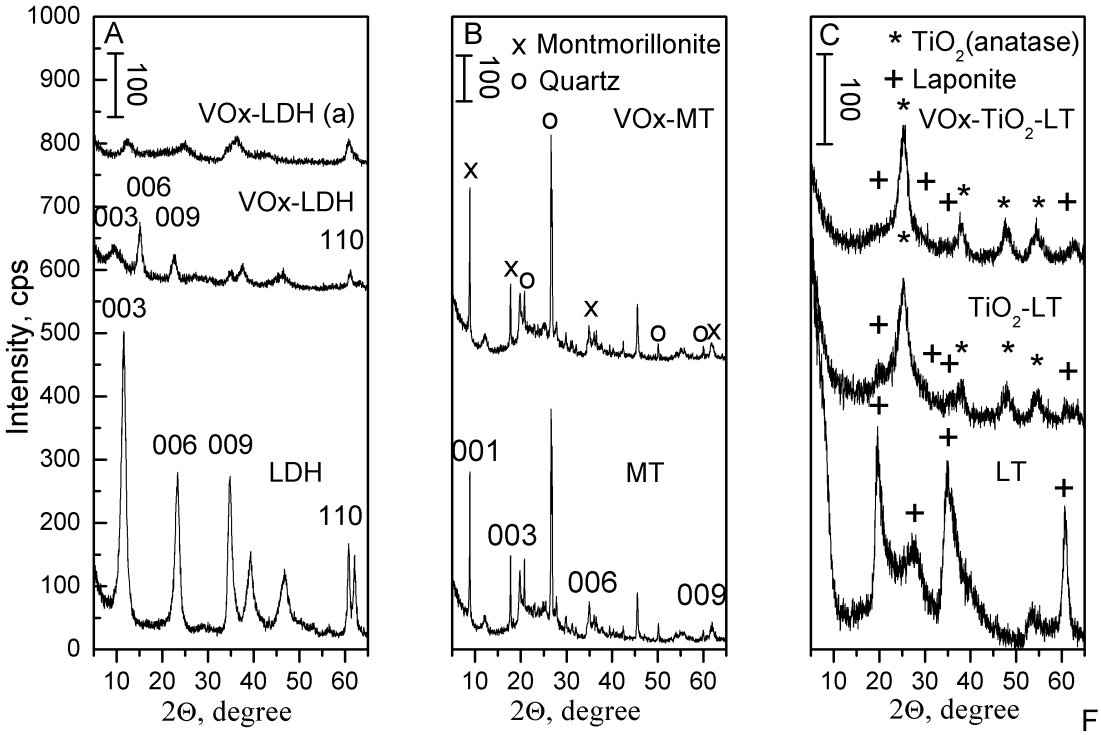

Fig 1.

Fig. 1. XRD patterns of layered and pillared layered materials recorded at room temperature. Section A shows the diffractogram of the LDH and VO_x-LDH sample after drying at 110°C overnight and the diffractogram of the VO_x-LDH(a) sample, obtained from the VO_x-LDH sample by heating it in air at 300 ^oC for 4 h. The diffractograms in sections B and C were recorded for samples activated in air at 400 ^oC for 3 h.

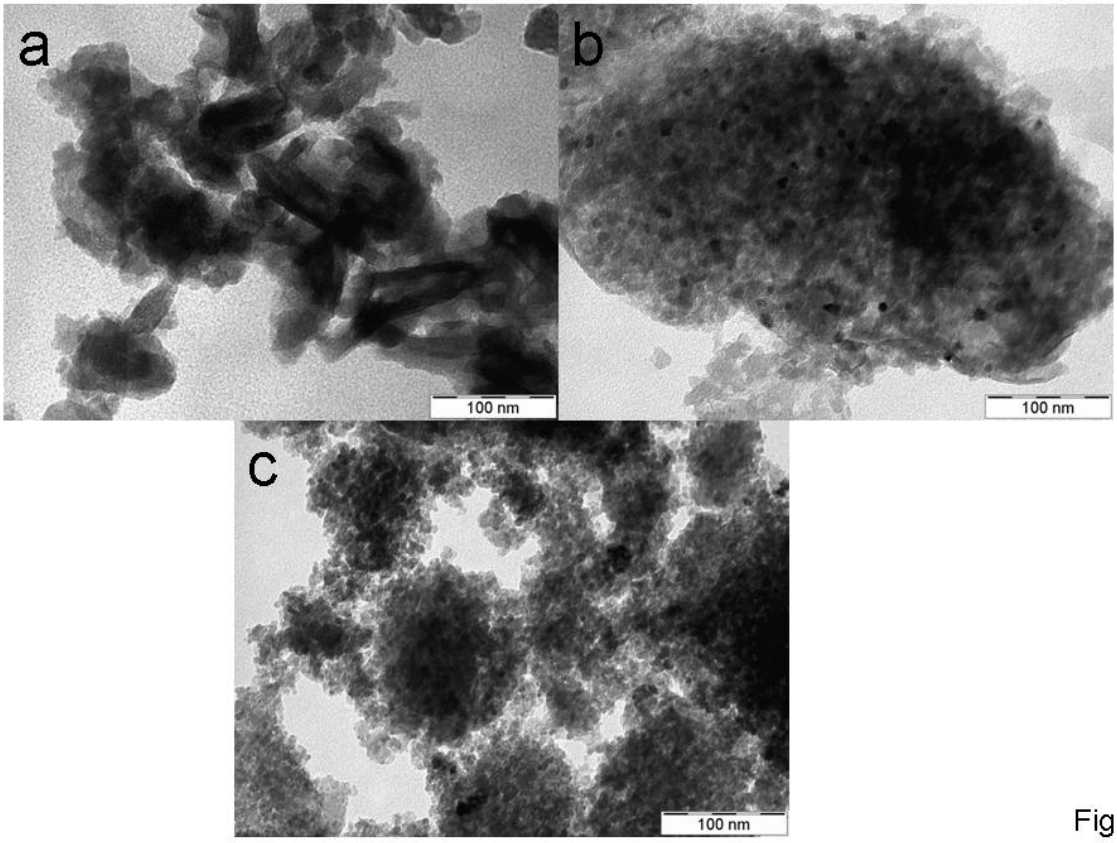

Fig. 2.

Fig. 2. TEM images of a) Pd/VOx-LDH, b) Pd/VOx-MT, c) Pd/VOx-TiO_2-LT. The LDH and the other catalysts were pre-calcined in air at 300^{o}C and 400 ^{o}C, respectively.

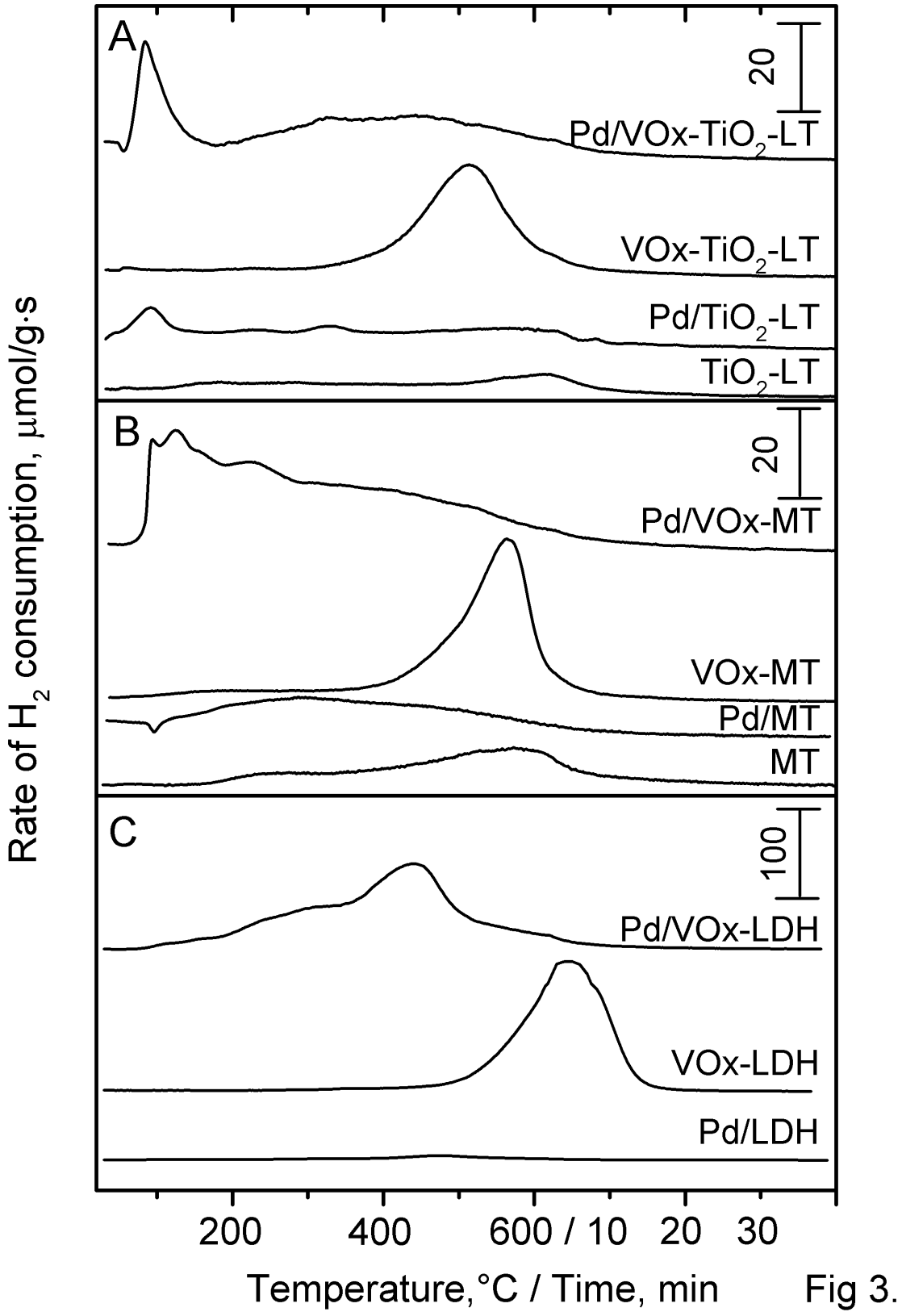

Fig. 3. H_2-TPR profiles of catalyst precursors and catalyst samples

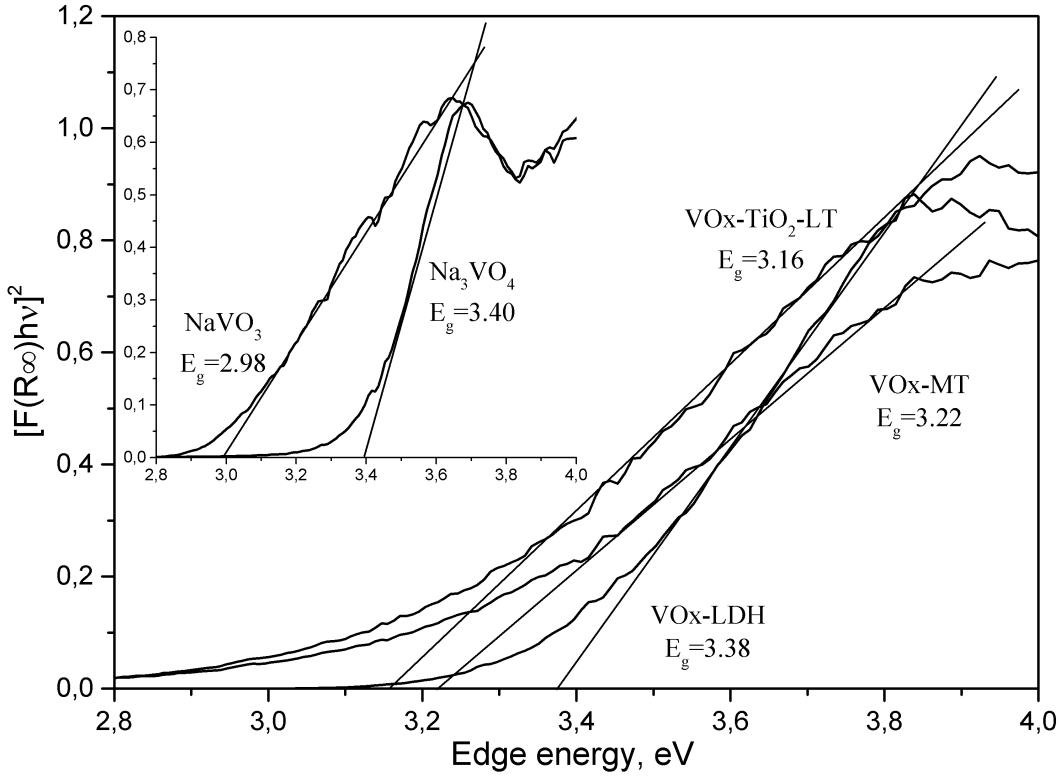

Fig. 4

Fig. 4. UV-vis DR spectra and E_g values of reference (insert) and catalyst materials. Both the background and absorbance data were collected at 350 °C after *in-situ* calcination at 350 °C in flowing oxygen for 30 min.

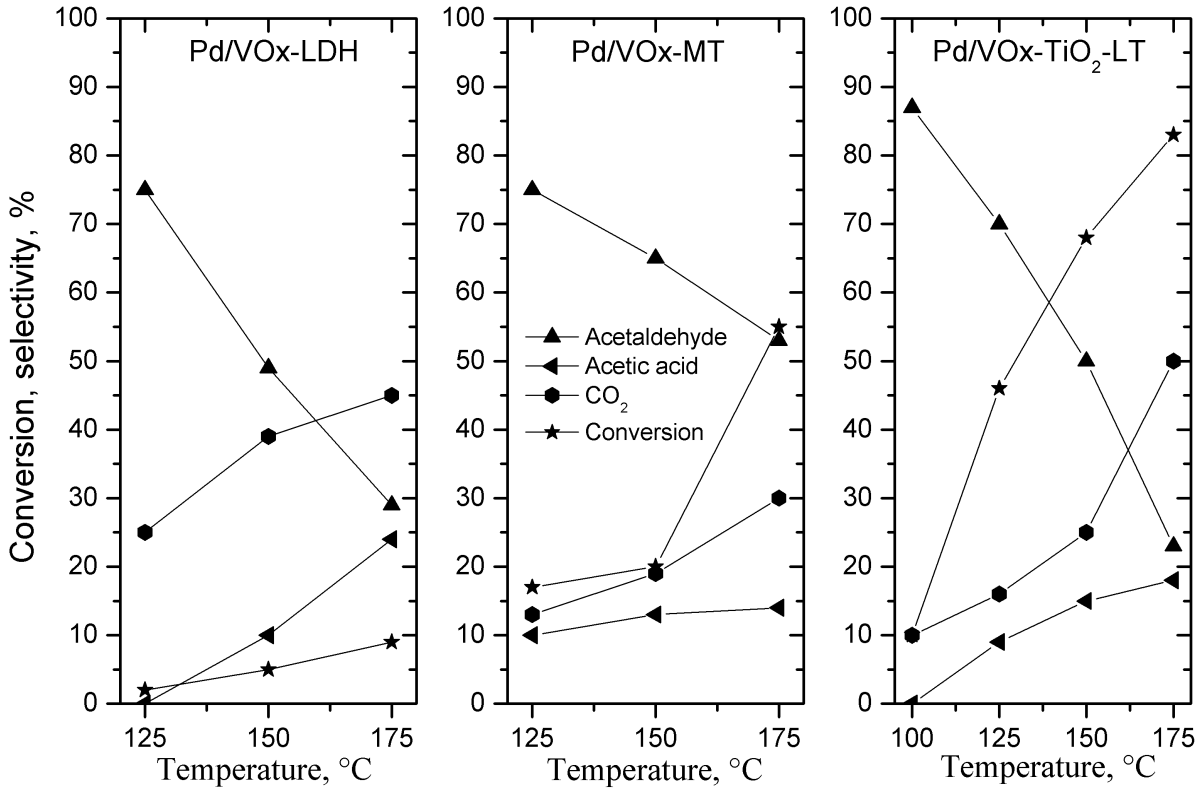

Fig. 5

Fig. 5. Catalytic conversion of 3% ethylene/12% oxygen/24% water/He gas mixture as a function of temperature over different catalysts The measurements were carried out at atmospheric pressure, GHSV= 3600 h^{-1} , conversions and selectivities were calculated from the ethylene consumption and on the basis of the carbon content of the products.

1. Hafner W, Jira R, Sedlmeier J, Sieber R, Rüttinger R, Kojer H (1959) Angew Chem 71:176
2. Park ED, Lee KH, Lee JS (2000) Catal Today 63:147
3. Evnin B, Rabo JA, Kasai PH (1973) J Catal 30, 109
4. Van der Heide E, Zwinkels M, Gerristen A, Scholten J (1992) Appl Cat A 86:181
5. Stobbe-Kreemers AW, Makkee M, Scholten JJF (1997) Appl Cat A 156:219
6. Park ED, Lee JS (1998) J Catal 180:123
7 Park ED, Lee JS (2000) J Catal 193:5
8. Dyakonov AJ (2003) Appl Catal B 45:257
9. Espeel PH, Tielen MC, Jacobs PA (1991) Chem Commun 10:669
10. Mitsudome T, Umetani T, Mori K, Mizugaki T, Ebitani K, Kaneda K (2006) Tetrahedron Lett 47:1425
11. Arhancet JP, Davis ME, Hanson BE (1991) Catal Lett 11:129
12. Okamoto M, Taniguchi Y (2009) J Catal 261:195
13. Frusteri F, Parmaliana A, Ostrovskii NM, Ianibello A, Giordano N (1997) Catal Lett 46:57
14. Long RQ, Yang RT (2000) J Catal 196:73
15. Węgrzyn A, Rafalska-Łasocha A, Dudek B, Dziembaj R (2006) Catal Today 116:74
16. Gao X, Wachs IE (2000) J Phys Chem B 104:1261

17. Tian H, Ross EI, Wachs IE (2006) J Phys Chem B 110:9593
18 Labajos FM, Rives V, Ulibarri,M.A (1992) J Mater Sci 27:1546
19 Forni L, Terzoni G (1977) Ind Eng Chem Process Des Dev 16 288
20 Grygar T, Čapek L, Adam J, Machovič V (2009) J Electroanal Chem 633:127
21 Gao X, Banares MA, Wachs IE (1999) J Catal 188:325
22 Pope D, Smith WL, Eastlake MJ, Moss RL (1971) J Catal 22:72
23 Smith WL (1972) J Appl Cryst 5:127